

An Approximate Carrier-Based Compact Model for Fully Depleted Surrounding-Gate MOSFETs with Finite Doping Body

Jin He^{*}, Feng Liu^{*}, Wei Bian^{*}, Yadong Tao^{*}, Wen Wu^{**}, Kailiang Lu^{**}, Ting Wang^{**}, and Mansun Chan^{**}

^{*} School of Computer & Information Engineering, Shenzhen Graduate School, Peking University, Shenzhen, 518055, P.R.China jinhe@ime.pku.edu.cn

^{**} Department of Electronic and Computer Engineering, Hong Kong University of Science & Technology, Clearwater Bay, Kowloon, Hong Kong

ABSTRACT

An approximate carrier-based compact model for fully depleted surrounding-gate MOSFETs with a finite doping body is developed in this paper. Starting from the Poisson's equation, the dopant effect is considered approximately by a superposition principle. The analytic surface potential is compared with 3-D device simulation and the error is also compared for different body doping. The analytic IV model is derived from the Pooh-Bah current equation under the gradual channel approximation and its predictions are verified by the 3-D simulation results of the fully-depleted SRG MOSFET devices for the finite body doping concentration less than 10^{17} cm^{-3} .

Keywords: Non-classical MOSFETs; Device physics; Compact modeling; Surrounding-gate MOSFET; Carrier-based model; Doping effects.

1 INTRODUCTION

In the recent works, a one-dimensional (1-D) Poisson equation was solved for the SRG MOSFET to derive analytical solution for surface potential, charge, and IV performance [1-4]. A basic feature of these compact modeling works is to use an undoped (or lightly doped) body assumption to sustain their theory results. The idea of an undoped body, sometimes referred to as "intrinsic channel", is expected to have special advantages such as the low leakage current, free-statistic dopant fluctuation, and improved short-channel effects. However, the practical SRG MOSFET is always a doped body structure due to a small order unintentional doping ($10^{12} \text{ cm}^{-3} \sim 10^{15} \text{ cm}^{-3}$) during the real fabrication process. Thus, the undoped body is only an ideal approximation for light and low-doped case in all non-classical CMOS device. The practical SRG device may be designed as a fully depleted MOSFET in order to take the advantages of the undoped body via the low body concentration process and materials. Since the dopant concentration does not only change the surface potential magnitude, but also strongly changes the device sub-threshold slope, an analytic doped SRG MOSFET model is highly desirable for the circuit design and performance test.

Following the carrier-based approach [7-8] and using a superposition principle, an approximate carrier-based compact model for the fully depleted SRG MOSFETs with a finite doping body is approximately developed directly from both the Poisson equation solution and the Pao-Sah current formulation. It is shown that this analytic model covers all three regions of SRG MOSFET operation in terms of the carrier concentration function, providing a continuous and physics based description of the SRG MOSFET characteristics.

2 MODEL DEVELOPMENT

This paper only discusses the fully depleted SRG n-channel MOSFET, thus, the hole is negligible. The standard cylindrical coordinate formulation of Poisson-Boltzmann equation in a doped SRG MOSFET is written as

$$\frac{d^2\phi}{dr^2} + \frac{1}{r} \frac{d\phi}{dr} = \frac{qN_a}{\epsilon_{si}} \left[1 + \left(\frac{n_i}{N_a} \right)^2 \exp(\beta(\phi - V)) \right] \quad (1)$$

Where n_i and N_a are the intrinsic silicon concentration and the body doping concentration in the silicon film with the unit of cm^{-3} , respectively ϵ_{si} and ϕ are the silicon dielectric constant and the electrostatic potential in Volt respectively. r is the cylindrical coordinate in cm along the radius direction of the silicon film? $1/\beta$ and V are the thermal voltage and the quasi-Fermi-potential in Volt. Boltzmann's statistics can be expressed

$$n = \frac{n_i^2}{N_a} \exp(\beta(\phi - V)) \quad n_0 = \frac{n_i^2}{N_a} \exp(\beta(\phi_0 - V)) \quad (2)$$

Where n_0 and ϕ_0 are the induced electron concentration in cm^{-3} and the electrostatic potential in V at $r = 0$. In a SRG MOSFET, the silicon radius center where the electric field is always zero is chosen as coordinate reference point.

It may be very difficult to get the closed-form surface potential solution following the traditional integration routine for (1) due to the non-linear coupled characteristics between the depletion charge and the induced electron charge. However, if only the mobile electron is considered in (1), the Poisson equation solution in terms of the carrier concentration can be written as [7-8]

$$\phi_s - \phi_{0I} = \frac{2}{\beta} \ln \left[1 - \frac{R^2}{8L_D^2} \frac{n_0}{N_a} \right] \quad (3)$$

Where ϕ_{sI} and ϕ_{0I} are the silicon surface and centric potentials in *Volt* contributed by the induced electron charge. $L_D = \sqrt{\epsilon_{si} kT / q^2 N_a}$ is the Debye length in cm of silicon film with doping concentration of N_a . Please note the logarithm function of Eq. (3) gives a limitation for the developed analytic model for the SRG MOSFET doping concentration and the silicon film radius as discussed in the following section.

Similarly, we obtain the inversion density from the carrier-based Poisson equation solution in [4-5]

$$Q_i = \frac{\epsilon_{si} R}{2\beta L_D^2} \frac{n_0 / N_a}{1 - \frac{R^2}{8L_D^2} \frac{n_0}{N_a}} \quad (4)$$

Where Q_i is the induced electron density in the silicon film in $C \cdot cm^{-2}$. If only the dopant is considered in (1) and the fully depletion approximation is used, the Poisson equation solution in the SRG can be written as

$$Q_b = \sqrt{q\epsilon_{si} N_a (\phi_s - \phi_0)} \quad (5)$$

$$\phi_{sB} - \phi_{0B} = \frac{q_b R}{4\epsilon_{si}} \quad (6)$$

Where Q_b is the depleted charge density in $C \cdot cm^{-2}$ in the silicon film contributed by the doping atom. ϕ_{sB} and ϕ_{0B} are the silicon surface and centric potentials in *V* contributed by the depletion charge density, respectively.

It is well known that the superposition principle only applies to the linear equations. The use of the superposition principle to an intrinsically nonlinear equation such as Eq. (1) must be handled with care. However, for a low doped body MOSFET device, e.g the fully depleted SRG MOSFET, the coupling effect between the depletion charge and inversion charge is not so strong, because they dominate the different device operation region, thus, the superposition principle is approximated validated as shown in the following comparison between the analytic solutions and the 3-D simulations. Assuming that the superposition principle is approximately valid, the complete channel potential and the charge equations can be obtained by (3) plus (6), thus $\phi_s = \phi_{sI} + \phi_{sB}$

$$\phi_s = \phi_0 + \sqrt{\frac{qN_a R^2}{16\epsilon_{si}}} (\phi_s - \phi_0) - \frac{2}{\beta} \ln \left[1 - \frac{R^2}{8L_D^2} \frac{n_0}{N_a} \right] \quad (7)$$

and (4) plus (5)

$$Q_{tot} = Q_b + Q_i = \sqrt{q\epsilon_{si} N_a (\phi_s - \phi_0)} + \frac{\epsilon_{si} R}{2\beta L_D^2} \frac{n_0 / N_a}{1 - \frac{R^2}{8L_D^2} \frac{n_0}{N_a}} \quad (8)$$

where ϕ_s and Q_{tot} are the total silicon surface potential in *V* and the total charge in

$C \cdot cm^{-2}$ contributed by the induced mobile electron charges and the depleted charges, respectively.

From (7), we can get the surface potential in terms of the carrier concentration.

$$\phi_s = \phi_0 + \left[\sqrt{\alpha^2 / 4 - \frac{2}{\beta} \ln \left[1 - \frac{R^2}{8L_D^2} \frac{n_0}{N_a} \right]} + \alpha / 2 \right]^2 \quad (9)$$

Where

$$\alpha^2 = \frac{qN_a R^2}{16\epsilon_{si}} \quad (10)$$

For the Gauss's law, the following relation must hold:

$$C_{ox} (V_{gs} - \Delta\phi - \phi_s) = Q_{tot} \quad (11)$$

Where $C_{ox} = \epsilon_{ox} / t_{oxeff}$ is the gate oxide capacitance in F/cm^2 , t_{oxeff} is the effective thickness of gate oxide of Surrounding-Gate structure, and can be expressed as $R \ln(1 + t_{ox}/R)$, where R and t_{ox} is the radius of the silicon film and real oxide thickness. $\Delta\phi = \phi_{ms} - \frac{1}{\beta} \ln \left[\frac{N_a}{n_i} \right]$ is the

traditional flat band voltage in *Volt* for p type body N-MOSFET. For the midgap metal gate and intrinsic silicon, $\Delta\phi = \phi_{ms} = 0$ while $\Delta\phi$ is a function of the doping concentration for the doping MOSFET.

Substituting (8) and (9) into (11), a complete analytic solution of the Poisson equation is obtained in terms of the carrier concentration

$$V_{gs} - \Delta\phi - V - 2\phi_s = \frac{1}{\beta} \ln \left(\frac{n_0}{N_a} \right) + \left[\sqrt{\alpha^2 / 4 - \frac{2}{\beta} \ln \left[1 - \frac{R^2}{8L_D^2} \frac{n_0}{N_a} \right]} + \frac{\alpha}{2} \right]^2 + \gamma \left[\sqrt{\alpha^2 / 4 - \frac{2}{\beta} \ln \left[1 - \frac{R^2}{8L_D^2} \frac{n_0}{N_a} \right]} + \frac{\alpha}{2} \right] + \frac{\epsilon_{si} R}{2\beta C_{ox} L_D^2} \frac{n_0 / N_a}{1 - \frac{R^2}{8L_D^2} \frac{n_0}{N_a}} \quad (12)$$

Where $\gamma = \frac{\sqrt{2q\epsilon_{si} N_a}}{C_{ox}}$ is the bulk bias factor.

(12) gives the closed form expression of electron concentration at the silicon film center as a function of bias conditions, dopant concentration, and geometry sizes. Along the channel direction, the Quasi-Fermi-Potential *V* varies from the source to the drain. So does the electron concentration n_0 . Following Pao-Sah model [6], integrating $I_{ds} dy$ from the source to the drain and expressing dV / dy as $(dV / dn_0)(dn_0 / dy)$, the drain current is written as

$$I_{DS} = \mu \frac{W}{L} \int_0^{V_{DS}} q_i dV = \mu \frac{W}{L} \int_{n_{0S}}^{n_{0D}} q_i(n_0) \frac{dV}{dn_0} dn_0 \quad (13)$$

Where n_{0S} and n_{0D} are solutions of (12) corresponding to $V = 0$ being the source end voltage and $V = V_{ds}$ being the drain end voltage, respectively. μ is the effective channel mobility of the SRG MOSFET in $cm^2 / V.s$. L and $W = 2\pi R$ are the effective channel length and width of the SRG MOSFET in cm, respectively. Note that the

dV/dy can also be expressed as a function of n_0 by differentiating (12). Substituting these factors into (13), integrating can be performed approximately yet analytically to yield:

$$I_{ds} = \mu \frac{W}{L} \int_0^{V_{DS}} q_i dV = \frac{4\pi\mu\epsilon_{si}}{L} \left(\frac{2}{\beta}\right)^2 f(n_0) \Big|_{n_{0d}}^{n_{0s}} \quad (14)$$

Where

$$f(n_0) = \frac{1}{2} \ln \left[1 - \frac{R^2 n_0}{8\epsilon_s^2 N_s} \right] + \frac{\left[\frac{\epsilon_s - 2\epsilon_s \ln \left(1 + \frac{t_{ox}}{R} \right)}{\epsilon_s} \right]}{\epsilon_s \left[1 - \frac{R^2 n_0}{8\epsilon_s^2 N_s} \right]} + \frac{\epsilon_s \ln \left(1 + \frac{t_{ox}}{R} \right)}{\epsilon_s \left[1 - \frac{R^2 n_0}{8\epsilon_s^2 N_s} \right]} + \frac{\beta (\alpha + \gamma)}{2} \sqrt{\alpha^2 / 4 - \frac{2}{\beta} \ln \left[1 - \frac{R^2 n_0}{8\epsilon_s^2 N_s} \right]} \quad (15)$$

3 RESULTS AND DISCUSSION

The fully depleted SRG MOSFET characteristics for all operation regions can be predicted from this compact yet continuous, analytic model. In order to test the developed model we simulated long channel SRG MOSFETs with a channel length of $1\mu\text{m}$ and silicon gate oxide thickness (t_{ox}) of 2 nm for comparison when mobility degradation and quantum-confinement mechanisms are turned off in the ISE device simulator. The constant mobility of $400 \text{ cm}^2/V.s$ is used in all calculation and simulation. In order to demonstrate that the analytic model predicts the effect of the doping concentration on the surface potential and MOSFET current in details compared with the 3-D numerical simulation, $V_{gs} - \Delta\phi$ is chosen as the voltage variable in all figures so to begin with a same zero surface potential for the different doping as done for the bulk MOSFET [7]. In the following numerical simulation, the 3-D simulation result can follow this zero surface potential reference by $V_{gs} - \Delta\phi$ as the voltage variable.

Fig.1a shows the comparison of the surface potential versus gate voltage curves for five different doped concentrations from the intrinsic undoped assumption, e.g. $1.45e10 \text{ cm}^{-3}$ up to the doping concentration 10^{17} cm^{-3} , as calculated with (9) and (12), compared with the 3-D simulation. It is observed that the surface potential predicted by the presented model demonstrates gradual saturation trend as does the bulk MOSFET while the centric potential always has a pinch-off potential, which can be obtained from the bound of the logarithm function in (7). It is important that the prediction of the channel electrostatic potentials with this approximate analytic model shows good agreement with the 3-D simulation. The further test also finds that the analytic model result coincides with the implicit model [1,4] for the intrinsic doping case. However, the implicit model [1,4] cannot predict the dependence of the channel potentials on the body doping concentration while the presented analytic model captures the correct channel potential variation with the doping concentration increase as the 3-D simulation result demonstrated in Fig.1a.

Fig.1 (b) shows the relative error of the surface potential prediction by the analytic model compared with the 3-D numerical simulation. It is found that for the relative error is within the order of $1e-3$ for the body doping concentration up to $1e16 \text{ cm}^{-3}$. However, the relative error increases with the increase of the body concentration for the given geometry parameters. For example, the relative error increases to the order of $1e-2$ for the doping concentration up to $1e17 \text{ cm}^{-3}$. Further test for the doping concentration and the silicon film radius found that this SRG MOSFET almost approaches the fully-depleted boundary of the device physics. A SRG MOSFET will be a partial depleted device above such a doping concentration and silicon radius. In fact, the developed analytic model only applies to the fully depleted SRG MOSFET analysis.

Fig.2a and 2b show the comparison of the centric potential versus gate voltage curves for four different doped concentrations from the intrinsic undoped, e.g. $1.45e10 \text{ cm}^{-3}$ to the doping concentration of $1e17 \text{ cm}^{-3}$ between the analytic model and 3-D simulation, and the resultant relative error. It is found that the centric potentials predicted by the analytic model are also shows in agreement with the 3-D simulation in Fig.2a. However, the relative error of the centric potential also rises with the increase of the body concentration although the relative error magnitude is within the order of $1e-3$ for most doping level from $1.45e10 \text{ cm}^{-3}$ up to $1e17 \text{ cm}^{-3}$. The cause behind this increased error is just the discussed above, the developed analytic model works well for a really fully-depleted SRG MOSFETs. It will lead to increased error for the device approaching to partial depleted operation.

Fig.3 shows the comparison of I_{ds} versus V_{GS} between the analytic solution (curves) and the 3-D simulation (symbols) for the different doping concentration. In this Figure, the SRG MOSFET current predicted by the analytic model shows a good match with the 3-D numerical simulation from the sub-threshold region to the strong inversion region for most doping concentrations. However, the drain current in the strong inversion has an increased deviation from the 3-D numerical simulation for the doping concentration of $1e17 \text{ cm}^{-3}$ in the body. This result can be explained by the deviation of the channel potential calculation compared with 3-D simulation, as discussed above. This proposed analytic model, however, shows a good agreement with 3-D numerical result for the fully-depleted SRG MOSFET with low body doping concentration such as $N_a < 1e16 \text{ cm}^{-3}$.

Fig.4 is $I_{ds}-V_{DS}$ curves calculated from the analytic model (solid curves), compared with the 3-D numerical simulation results (open stars) of a long-channel doped surrounding-gate MOSFET. It is shown that the I-V curves constructed by the analytic model are in complete agreement with 3-D numerical simulation results of a fully-depleted SRG MOSFET devices for the finite body doping concentration $5e15 \text{ cm}^{-3}$ without fitting terms or parameters.

As mentioned above, this model does not account for the partially depleted case, thus will lead to some errors when it is used for the high doped concentration, e.g. up to $1e17cm^{-3}$ due to the partially depleted characteristic of the SRG MOSFET. Such a case, however, is not preferable in the non-classical CMOS devices, e.g. the SRG MOSFET design since the high body doping concentration will lead to strong statistics fluctuation effect and mobility degradation.

4 CONCLUSIONS

In summary, a carrier-based compact model for the fully-depleted surrounding-gate MOSFETs with the finite doped body has been derived in this paper by solving Poisson-Boltzmann equation and Pao-Sah current formulation approximated. All the regions of operation and the transitions of the fully-depleted SRG MOSFETs are correctly described by single set of the carrier equations. It is also shown that the model predicted I-V curves are in complete agreement with the 3-D numerical simulation results of the fully-depleted SRG MOSFET devices for the finite body doping concentration less than $10^{17}cm^{-3}$, with acceptable error.

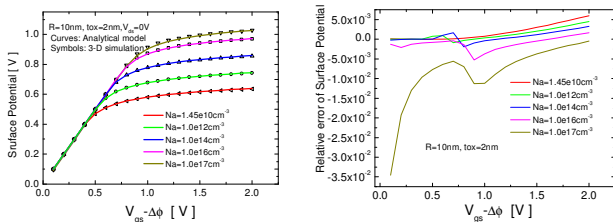


Fig.1: The comparison of the surface versus gate bias curves for different body doping concentration and error, calculated from the presented analytic model (solid curves), and extracted from the 3-D simulation of the ISE (symbols), for a N-channel SRG MOS capacitance..

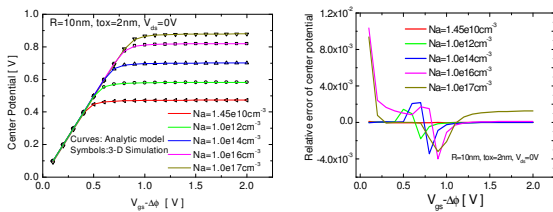


Fig.2: The comparison of the centric potential versus gate bias curves for different body doping concentration and error, calculated from the presented analytic model (solid curves), and extracted from the 3-D simulation of the ISE (symbols), for a SRG MOS capacitance.

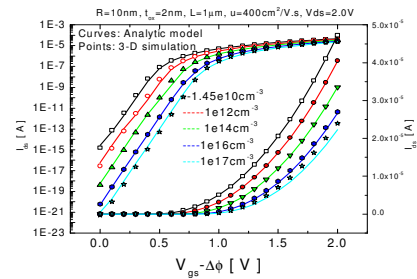


Fig.3: The comparison of the drain current versus gate bias curves for different body doping concentration calculated from the presented analytic model (solid curves) and extracted from the 3-D simulation of the ISE (symbols), for a SRG MOSFET.

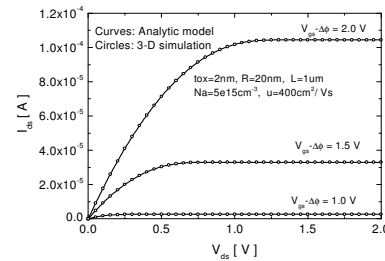


Fig.4: I_{ds} - V_{DS} curve calculated from the analytic model (solid curves), compared with the 3-D numerical simulation result (symbols), for a long channel SRG MOSFETs.

REFERENCES

- [1] D. Jiménez, et al., "Continuous analytical current-voltage model for surrounding-gate MOSFETs." IEEE EDL-25, No.8, pp. 571-573, 2004.
- [2] B. Iníguez, et al. "Explicit continuous model for long-channel undoped surrounding-gate MOSFETs." IEEE on Trans Electron Devices, TED-52 (8), pp.1868-1873, 2005.
- [3] Jin He, et al., "physics based analytical solution to undoped cylindrical surrounding-gate (SRG) MOSFETs." 5th IEEE Int. Caracas Conf. on Devices, Circuits and Systems, Nov.3-5, pp. 26-28, 2004.
- [4] Jin He, et al., "A complete carrier-based non-charge-sheet analytic theory for nano-scale undoped surrounding-gate MOSFETs". Proceedings of ISQED'2006, pp.115-120, San Jose, Mar. 28, 2006.
- [5] Jin He, et al. "A carrier-based analytic model for the undoped (lightly doped) cylindrical surrounding-gate MOSFETs." Solid-State Electronics, vol.50, No.3, pp. 416-421, 2006.
- [6] H. C. Pao, et al., "Effects of diffusion current on characteristics of metal-oxide (insulator)-semiconductor transistors," Solid-State Electronics, vol. 9, pp. 927-937, 1966.
- [7] N. Arora, MOSFET models for VLSI circuit simulation: theory and simulation, New York: Springer-Verlag, 1993.